THE JOURNAL OF PHYSICAL CHEMISTRY Letters

Letter

pubs.acs.org/JPCL

Accurate Quasiparticle Spectra from the T-Matrix Self-Energy and the Particle−Particle Random Phase Approximation

Du Zhang,[†] Neil Qiang Su,[†] and Weitao Yang*[,†,‡]

[†]Department of Chemistry, Duke University, Durham, North Carolina 27708, United States

[‡]Key Laboratory of Theoretical Chemistry of Environment, School of Chemistry and Environment, South China Normal University, Guangzhou 510006, China

Supporting Information

ABSTRACT: The *GW* self-energy, especially G_0W_0 based on the particle−hole random phase approximation (phRPA), is widely used to study quasiparticle (QP) energies. Motivated by the desirable features of the particle−particle (pp) RPA compared to the conventional phRPA, we explore the pp counterpart of *GW*, that is, the T-matrix self-energy, formulated with the eigenvectors and eigenvalues of the ppRPA matrix. We demonstrate the accuracy of the T-matrix method for molecular QP energies, highlighting the importance of the pp channel for calculating QP spectra.

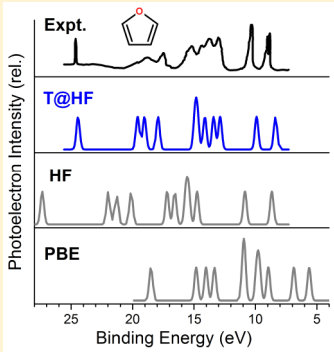

Kohn−Sham (KS) density functional theory (DFT)[1,2] calculations have been routinely performed in both materials and molecular applications. Its success is made possible by the development of accurate density functional approximations (DFAs)[3−9] to the exact exchange−correlation (xc) energy functional. Despite the popularity of DFT, most DFAs yield underestimated band gaps,[10−13] which originate from the delocalization error,[14,15] namely, their deviation from the linearity condition of fractional charges in finite systems.[16−18] Also, for systems with strong static correlation, common DFAs tend to greatly overestimate the total energies, deviating from the energy constancy condition of fractional spins.[18−20] Combining these two exact conditions, the total energy flat-plane condition has been formulated[21] and has guided recent development such as the local scaling correction[22] and the particle−particle random phase approximation (ppRPA).[23,24] In particular, the ppRPA is the first DFA that satisfies the flat-plane condition. In contrast, the conventional particle−hole (ph) RPA has major deviations.

(Generalized) KS orbital energies obtained from common DFAs are not good approximations in general to quasiparticle (QP) energies because of the delocalization error.[14,15] One popular approach of obtaining QP energies is the *GW* approximation,[25] performed as a post-DFT procedure and often with the phRPA screened interaction. It has been extensively applied to calculating the QP band structure for solids[11,26] and more recently to obtaining molecular ionization potentials (IPs).[27−30] *GW* QP energies show significant improvement over DFA orbital energies as compared to experimental data. Efforts of incorporating vertex effects have been made by adding the contribution of the exchange correlation kernel f_{xc} (the second functional derivative of the xc energy functional approximation).[11,31−33] Another route is the summation of ladder diagrams from the pp channel rather than the direct ring diagrams from the ph channel, yielding the Bethe−Goldstone approximation or the T-matrix approximation,[34−38] first introduced for the nuclear many-body problem. It has also been applied to calculating the electronic structure of the Hubbard model.[39−42] For the electron gas, the T-matrix approximation is justified in the low-density limit,[37,43] while the phRPA is correct for the high-density limit.[44] The combination of correlation channels has also been achieved and applied to electronic structure calculations for the Hubbard model[45] and strongly correlated metals.[43,46−48]

Motivated by the desirable behavior of the ppRPA as compared to the phRPA in terms of thermochemistry as well as the satisfaction of the flat-plane condition,[23,24] we now extend the application of the post-ppRPA T-matrix self-energy to molecular electronic structure for the first time, computing IPs and electron affinities (EAs) of atoms and molecules. This is achieved by formulating the working equation of the T-matrix self-energy in terms of the eigenvalues and eigenvectors of the ppRPA matrix. The self-energy correction to orbital energies is then performed as a post-ppRPA step. Comparison is made with existing methods including the *GW* approximation.

The key quantity is the many-body self-energy. At the first order, the direct contribution $\Sigma_d^{(1)}$ and exchange contribution $\Sigma_x^{(1)}$ correspond to the local Hartree potential and the nonlocal

Received: May 22, 2017
Accepted: June 27, 2017
Published: June 27, 2017

DOI: 10.1021/acs.jpclett.7b01275
J. Phys. Chem. Lett. 2017, 8, 3223−3227

Table 1. MSEs and MAEs of Computed HOMO IPs of 26 Small Systems from Experimental Data[29,30,60a]

			second-order @		T-matrix @		G_0W_0@		
	HF	PBE	HF	PBE	HF	PBE	HF	PBE	*GW*
MSE	0.81	−4.90	−0.48	−2.90	−0.15	−1.29	−0.19	−0.19	−0.43
MAE	0.91	4.90	0.56	2.90	0.31	1.29	0.36	0.41	0.52

[a]Molecular structures are from the G3 set[61,62] and ref 29; reported results of self-consistent *GW* (*GW*) and G_0W_0 with the HF (G_0W_0@HF) and PBE (G_0W_0@PBE) references are from refs 27 and 30 (units: eV).

Fock exchange potential. The second-order self-energy also contains a direct contribution $\Sigma_d^{(2)}$ and an exchange contribution $\Sigma_x^{(2)}$, but unlike the first-order contributions, it is nonlocal in time.

In the ph channel, the G_0W_0 approximation is the infinite summation of direct ring diagrams. Its time-domain real-space analytical expression is given by[49]

$$\Sigma_{xc}^{G_0W_0}(1, 2) = iG_0(1, 2)W_0(1, 2) \tag{1}$$

The variables 1, 2, etc., stand for the combined space−time−spin variables. Fourier transform into the frequency domain and projection onto MO space yield the expression for the correlation part of the G_0W_0 self-energy in terms of the eigenvectors and eigenvalues of the phRPA matrix.[29] An alternative expression that bypasses the diagonalization of the phRPA matrix involves imaginary frequency integration. It can be combined with the resolution-of-identity technique for computational speed-up, as was performed in calculating molecular IPs and EAs by Ke.[28]

In the pp channel, the infinite summation of ladder diagrams plus their corresponding exchange terms leads to the T-matrix approximation. The RHS of the equality shows the infinite sum as the one-particle Green's function G_0 multiplied by a four-point interaction obtained from solving the ppRPA equation, and the corresponding time-domain real-space expression is given by[50]

$$\Sigma_{Hxc}^{T}(1, 2) = i\int d3\, d4\, G_0(4, 3)T_0(1, 3; 2, 4) \tag{2}$$

where, unlike the two-point screened interaction W_0 from the phRPA, the T_0 matrix from the ppRPA is a generalized four-point effective interaction. In contrast to the G_0W_0 approximation, the T-matrix approximation is exact up to second order because of its proper treatment of the exchange terms describing the Fermionic nature of electrons. Fourier transform into the frequency domain and projection onto MO space yield the following expression for the correlation part of the T-matrix self-energy (see the Supporting Information (SI))

$$\Sigma_c^{T}(p, q; \omega) = \sum_m \sum_i \frac{\langle pi|\chi_m^{N+2}\rangle\langle qi|\chi_m^{N+2}\rangle}{\omega + \epsilon_i - \omega_m^{N+2}} + \sum_m \sum_a \frac{\langle pa|\chi_m^{N-2}\rangle\langle qa|\chi_m^{N-2}\rangle}{\omega + \epsilon_a - \omega_m^{N-2}} \tag{3}$$

where

$$\langle pi|\chi_m^{N+2}\rangle = \sum_{c<d}\langle pi||cd\rangle X_{cd}^{N+2,m} + \sum_{k<l}\langle pi||kl\rangle Y_{kl}^{N+2,m} \tag{4}$$

$$\langle pa|\chi_m^{N-2}\rangle = \sum_{c<d}\langle pa||cd\rangle X_{cd}^{N-2,m} + \sum_{k<l}\langle pa||kl\rangle Y_{kl}^{N-2,m} \tag{5}$$

The above equations use the antisymmetrized two-electron integral in the physicist's notation (see the SI). $X_{cd}^{N\pm2,m}$ and $Y_{kl}^{N\pm2,m}$ are the double-electron addition/removal eigenvector components for the ppRPA matrix[51]

$$\begin{bmatrix} \mathbf{A} & \mathbf{B} \\ \mathbf{B}^{T} & \mathbf{C} \end{bmatrix}\begin{bmatrix} \mathbf{X}^{N\pm2,m} \\ \mathbf{Y}^{N\pm2,m} \end{bmatrix} = \omega_m^{N\pm2}\begin{bmatrix} \mathbf{X}^{N\pm2,m} \\ -\mathbf{Y}^{N\pm2,m} \end{bmatrix} \tag{6}$$

where the matrix elements are given in SI. Equation 3 is the key development in this work. We point out that in order to bypass the $O(N^6)$ formal scaling in our current working equation, the equivalent imaginary frequency integration formulation is preferred, just as in the G_0W_0 case. For the pp-RPA correlation energy calculations in particular, the tensor hypercontraction technique can be applied to bring down the complexity to a formal $O(N^4)$.[52] The corresponding development for the T-matrix self-energy is under active investigation.

With the self-energy approximations, IPs, EAs, and other QP energies can be calculated with the diagonal QP energy correction formula

$$\epsilon_p^{QP} = \epsilon_p^{SCF} + Z_p[\Sigma(p, p; \epsilon_p^{SCF}) - \langle p|v_{xc}|p\rangle] \tag{7}$$

where $Z_p = \left(1 - \frac{\partial\Sigma(p,p;\omega)}{\partial\omega}\Big|_{\omega=\epsilon_p^{SCF}}\right)^{-1}$. The self-energy Σ contains the exchange and correlation terms, and $\langle p|v_{xc}|p\rangle$ stands for the diagonal exchange−correlation potential matrix element from a DFA.

The HF, PBE, second-order self-energy, and post-ppRPA T-matrix calculations are performed with QM^{4}D.[53] The HF and PBE references are used for the T-matrix and second-order self-energy calculations. The cc-pVTZ basis set[54,55] is used for all IP calculations except the case of furan, for which the aug-cc-pVDZ basis set[56] is used; the cc-pVTZ + Dunning−Hay (DH) double Rydberg basis set (for elements other than H, Li, and Na), the cc-pVTZ + DH diffuse basis set (for H and Li),[57] and the cc-pVTZ basis set (for Na) are used for the LUMO EA calculations. For further details about the basis set convergence behavior refer to Table 1 of the SI and discussions therein.

First we present the HOMO IPs of 26 small systems (Table 1 and Figure 1a,b; Table 2 of the SI for numerical values of each system). The PBE eigenvalues hugely underestimate the HOMO IPs, with a mean signed error (MSE) of −4.90 eV (Table 1). This should not be surprising given the large delocalization errors of common DFAs under the generalized gradient approximation (GGA). Moreover, the QP correction results with the PBE reference for the second-order and T-matrix self-energies also give MSEs of −2.90 and −1.29 eV, respectively. We ascribe this to the poor PBE reference orbitals and their energies. When the reference is inferior, the validity of the QP correction formula, essentially a first-order perturbative formula with an extra normalization factor Z_p, becomes less reliable. Z_p partially accounts for the higher-order effects. The

DOI: 10.1021/acs.jpclett.7b01275
J. Phys. Chem. Lett. 2017, 8, 3223−3227

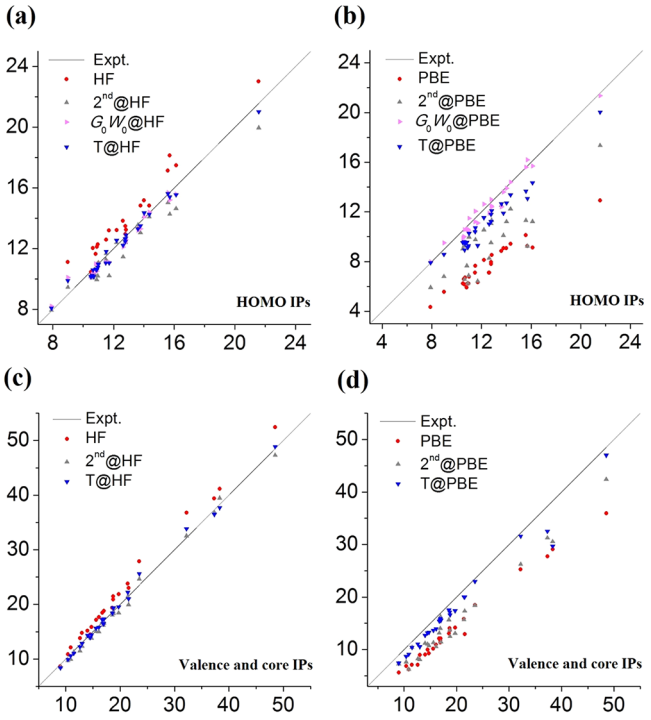

Figure 1. Computed IPs (*y*-axis) plotted against experimental values (*x*-axis) (unit: eV): HOMO IPs of 26 small molecules estimated from (a) HF-reference and (b) PBE-reference; valence and core IPs of 7 small molecules estimated from (c) HF-reference and (d) PBE-reference. Numerical values are listed in Tables 1 and 3 and in Tables 2 and 4 of the SI.

closer Z_p is to 1, the less important the higher-order contributions are, and thus, the better converged is the perturbative QP correction. Compared to PBE, although the HF eigenvalues systematically overestimate the HOMO IPs because of localization error,[14,15] the MSE is only 0.81 eV. Particularly, for F_2, the PBE HOMO IP (9.24 eV) deviates significantly from the experimental value (15.70 eV), while the HF HOMO IP (18.14 eV) deviates less. The Z_p's in the QP correction for the T-matrix HOMO IPs are 0.927 (HF reference) and 0.859 (PBE reference). Accordingly, the T-matrix HOMO IP with the HF reference (15.40 eV) reproduces the experimental value much better than does the PBE reference result (13.08 eV).

Notably, the T-matrix results appear more dependent on the SCF reference than do the G_0W_0 results. The T-matrix results with the PBE reference display a much larger MSE and MAE than those with the HF reference (Table 1). A similar situation is observed at the second order (Table 1). The better performance of the HF reference is likely a result of the more desirable properties of the HF orbitals and orbital energies than their DFT counterparts.[58,59] Overall, the T-matrix results with the HF reference show the least dispersion from the experimental data (Figure 1) among all of the methods studied, yielding the smallest MAE (0.31 eV) and MSE (−0.15 eV). In comparison, the G_0W_0 results with the HF reference, the most robust of the considered *GW* schemes for our tested systems, have a larger mean absolute error (MAE) (0.36 eV) and MSE (−0.19 eV).

Then we examine the LUMO EAs for eight small molecules (Table 2). As recommended in ref 66, the DH double Rydberg or diffuse basis functions are added to achieve better converged EAs. For IPs, however, the effect of the DH basis functions is insignificant[66] (also see the SI). The results are compared with both literature benchmark[30,60] and CCSD(T) total energy differences calculated with the same basis set. The discrepancy between the CCSD(T) results (Table 3 of the SI) and the reference benchmark data is most likely associated with the basis set effect, which stands out for F_2 in particular. The two sets of G_0W_0@PBE results are not very consistent, also indicating the basis set dependence.[30] In terms of accuracy, the second-order self-energy with the HF reference yields the smallest MAE, while the T-matrix data with the HF reference and the two sets of G_0W_0@PBE results are similar but worse than the HF orbital energies. As in the case of HOMO IPs, the second-order and T-matrix results with the PBE reference show significantly greater MAEs due to the poor PBE starting point. Overall, the LUMO EA predictions are less satisfactory than HOMO IPs, for both the T-matrix and G_0W_0 approximations. Also, unlike the IPs, the EAs are strongly dependent on the basis set. However, because the G_0W_0 method is in general successful in solid-state applications despite the apparent challenge in predicting accurate molecular EAs here, we remain cautiously optimistic about the expected performance of our

Table 2. Experimental and Computed LUMO Energies of Small Molecules[a]

				second-order @		T-matrix @		G_0W_0@PBE	
sys.	ref	HF	PBE	HF	PBE	HF	PBE	TM	BGW
LiH	0.34	0.20	1.64	0.28	0.12	0.26	−0.08	0.07	0.37
BH_3[b]	0.04	−0.08	3.06	−0.08	1.01	−0.08	−0.14	−0.12	0.06
NaCl	0.73	0.57	2.30	0.66	0.44	0.64	0.26	0.39	1.38
BN[c]	3.16	2.96	7.27	3.84	5.08	3.94	3.96	3.95	3.99
CS_2	0.01	−0.06	2.85	−0.05	1.01	−0.05	0.64	0.20	0.43
O_3	1.93	1.62	6.38	1.93	1.91	2.80	3.25	2.30	2.59
SO_2	0.81	0.21	4.74	1.03	1.02	1.28	1.76	1.00	1.24
F_2	0.42	−0.08	5.89	−0.08	2.04	−0.08	2.01	0.70	0.41
MSE		−0.26	3.34	0.02	0.65	0.16	0.53	0.13	0.38
MAE		0.26	3.34	0.21	0.78	0.37	0.79	0.32	0.38

[a]Reference vertical EAs are taken from ref 30 for LiH, BH_3, NaCl, and BN and from ref 60 for CS_2, O_3, SO_2, and F_2; molecular structures are from the G3 set[61,62] unless otherwise specified; two sets of reference G_0W_0@PBE results[30] are presented, one obtained with TURBOMOLE (TM) and the other with Berkeley*GW* (BGW). The last two rows show the MSEs and MAEs with respect to the reference data (units: eV). [b]The bond length of the D_{3h} BH_3 was taken as 1.19 Å.[63] [c]The bond length of BN was taken as 1.281 Å.[64]

DOI: 10.1021/acs.jpclett.7b01275
J. Phys. Chem. Lett. 2017, 8, 3223−3227

post-ppRPA T-matrix method in solid band structure calculations.

Table 3. MSEs and MAEs of Computed Valence and Core and IPs for Seven Small Molecules from Experimental Data[65] (units: eV)

			second-order @		T-matrix @	
	HF	PBE	HF	PBE	HF	PBE
MSE	1.56	−5.83	−0.46	−4.38	0.01	−1.90
MAE	1.67	5.83	0.62	4.38	0.54	1.90

Finally, consider the valence and core IPs for seven small systems (Table 3, Figure 1c,d; Table 4 of the SI for numerical values of each system). As in the case of the HOMO IPs, the HF eigenvalues systematically overestimate the core IPs as well (Figure 1c), while the PBE IPs are too low (Figure 1d). Under the diagonal QP correction approximation, the second-order self-energy with the HF reference slightly overcorrects the HF eigenvalues, with an MSE of −0.46 eV. The T-matrix method with the HF reference presents the smallest MSE of 0.01 eV. In terms of the MAE, the performance of the T-matrix approximation with the HF reference is the most robust (Table 3), closely followed by the second-order self-energy with the HF reference. With the PBE reference, the T-matrix results offer significant improvement over the PBE eigenvalues although still underestimating the experimental IPs, while the second-order self-energy offers only a modest improvement (Figure 1d).

In summary, we have developed the working equations for computing the QP spectra of atoms and molecules with the T-matrix self-energy. This has been achieved using a QP energy correction procedure followed by a ppRPA calculation, similar to the G_0W_0 calculation based on the phRPA. The G_0W_0 and T-matrix approximations correspond to the diagrammatic summation of self-energy terms in the ph and pp channels, respectively. Compared with the G_0W_0 approximation, the performance of the T-matrix approximation with the HF reference is superior for HOMO IPs and similar for LUMO EAs. For core IPs, the T-matrix approximation also delivers significant improvement over the HF and PBE orbital energies as well as the second-order self-energy results on top of them. Regarding future applications to extended systems, the greater importance of the ph screening channel may make it insufficient to account for the pp pairing correlation channel alone. Nevertheless, on the basis of the robust behavior of the post-ppRPA T-matrix method in molecular systems, we expect that the explicit consideration of pp channel correlation contributions beyond the conventional ph channel may also benefit solid-state applications.

■ ASSOCIATED CONTENT

Supporting Information

The Supporting Information is available free of charge on the ACS Publications website at DOI: 10.1021/acs.jpclett.7b01275.

Detailed mathematical derivations and calculation results (PDF)

■ AUTHOR INFORMATION

Corresponding Author

*E-mail: weitao.yang@duke.edu.

ORCID

Weitao Yang: 0000-0001-5576-2828

Notes

The authors declare no competing financial interest.

■ ACKNOWLEDGMENTS

D.Z. and N.S. appreciate the support as part of the Center for the Computational Design of Functional Layered Materials, an Energy Frontier Research Center funded by the U.S. Department of Energy, Office of Science, Basic Energy Sciences under Award # DE-SC0012575. D.Z. also acknowledges the support of the Joe Taylor Adams Fellowship from Duke University. W.Y. appreciates the support from the National Science Foundation (CHE-1362927).

■ REFERENCES

(1) Hohenberg, P.; Kohn, W. Inhomogeneous Electron Gas. *Phys. Rev.* **1964**, *136*, B864−B871.

(2) Kohn, W.; Sham, L. J. Self-consistent Equations Including Exchange and Correlation Effects. *Phys. Rev.* **1965**, *140*, A1133.

(3) Becke, A. D. Density-Functional Exchange-Energy Approximation with Correct Asymptotic Behavior. *Phys. Rev. A: At., Mol., Opt. Phys.* **1988**, *38*, 3098.

(4) Lee, C.; Yang, W.; Parr, R. G. Development of the Colle-Salvetti Correlation-Energy Formula into a Functional of the Electron Density. *Phys. Rev. B: Condens. Matter Mater. Phys.* **1988**, *37*, 785.

(5) Becke, A. D. Density-Functional Thermochemistry. I. The Effect of the Exchange-Only Gradient Correction. *J. Chem. Phys.* **1992**, *96*, 2155.

(6) Becke, A. D. Density-Functional Thermochemistry. III. The Role of Exact Exchange. *J. Chem. Phys.* **1993**, *98*, 5648−5652.

(7) Perdew, J. P.; Burke, K.; Ernzerhof, M. Generalized Gradient Approximation Made Simple. *Phys. Rev. Lett.* **1996**, *77*, 3865−3868.

(8) Perdew, J. P.; Burke, K.; Ernzerhof, M. ERRATA: Generalized Gradient Approximation Made Simple. *Phys. Rev. Lett.* **1997**, *78*, 1396.

(9) Sun, J.; Ruzsinszky, A.; Perdew, J. P. Strongly Constrained and Appropriately Normed Semilocal Density Functional. *Phys. Rev. Lett.* **2015**, *115*, 036402.

(10) Perdew, J. P.; Zunger, A. Self-Interaction Correction to Density-Functional Approximations for Many-Electron Systems. *Phys. Rev. B: Condens. Matter Mater. Phys.* **1981**, *23*, 5048.

(11) Hybertsen, M. S.; Louie, S. G. Electron Correlation in Semiconductors and Insulators: Band Gaps and Quasiparticle Energies. *Phys. Rev. B: Condens. Matter Mater. Phys.* **1986**, *34*, 5390−5413.

(12) Paier, J.; Marsman, M.; Hummer, K.; Kresse, G.; Gerber, I. C.; Ángyán, J. G. Screened Hybrid Density Functionals Applied to Solids. *J. Chem. Phys.* **2006**, *124*, 154709.

(13) Heyd, J.; Peralta, J. E.; Scuseria, G. E.; Martin, R. L. Energy Band Gaps and Lattice Parameters Evaluated with the Heyd-Scuseria-Ernzerhof Screened Hybrid Functional. *J. Chem. Phys.* **2005**, *123*, 174101.

(14) Mori-Sanchez, P.; Cohen, A. J.; Yang, W. Localization and Delocalization Errors in Density Functional Theory and Implications for Band-Gap Prediction. *Phys. Rev. Lett.* **2008**, *100*, 146401.

(15) Cohen, A. J.; Mori-Sánchez, P.; Yang, W. Fractional Charge Perspective on the Band Gap in Density-Functional Theory. *Phys. Rev. B: Condens. Matter Mater. Phys.* **2008**, *77*, 115123.

(16) Perdew, J. P.; Parr, R. G.; Levy, M.; Balduz, J. L., Jr Density-Functional Theory for Fractional Particle Number: Derivative Discontinuities of the Energy. *Phys. Rev. Lett.* **1982**, *49*, 1691.

(17) Cohen, A. J.; Mori-Sanchez, P.; Yang, W. Development of Exchange-Correlation Functionals with Minimal Many-Electron Self-Interaction Error. *J. Chem. Phys.* **2007**, *126*, 191109.

(18) Cohen, A. J.; Mori-Sánchez, P.; Yang, W. Insights into Current Limitations of Density Functional Theory. *Science* **2008**, *321*, 792−794.

DOI: 10.1021/acs.jpclett.7b01275
J. Phys. Chem. Lett. 2017, 8, 3223−3227

(19) Cohen, A. J.; Mori-Sanchez, P.; Yang, W. Fractional Spins and Static Correlation Error in Density Functional Theory. *J. Chem. Phys.* **2008**, *129*, 121104.
(20) Cohen, A. J.; Mori-Sánchez, P.; Yang, W. Challenges for Density Functional Theory. *Chem. Rev.* **2012**, *112*, 289−320.
(21) Mori-Sanchez, P.; Cohen, A. J.; Yang, W. Discontinuous Nature of the Exchange-Correlation Functional in Strongly Correlated Systems. *Phys. Rev. Lett.* **2009**, *102*, 066403.
(22) Li, C.; Zheng, X.; Cohen, A. J.; Mori-Sánchez, P.; Yang, W. Local Scaling Correction for Reducing Delocalization Error in Density Functional Approximations. *Phys. Rev. Lett.* **2015**, *114*, 053001.
(23) van Aggelen, H.; Yang, Y.; Yang, W. Exchange-Correlation Energy from Pairing Matrix Fluctuation and the Particle-Particle Random-Phase Approximation. *Phys. Rev. A: At., Mol., Opt. Phys.* **2013**, *88*, 030501.
(24) Yang, Y.; van Aggelen, H.; Steinmann, S. N.; Peng, D.; Yang, W. Benchmark Tests and Spin Adaptation for the Particle-Particle Random Phase Approximation. *J. Chem. Phys.* **2013**, *139*, 174110.
(25) Hedin, L. New Method for Calculating the One-Particle Green's Function with Application to the Electron-Gas Problem. *Phys. Rev.* **1965**, *139*, A796−A823.
(26) Onida, G.; Reining, L.; Rubio, A. Electronic Excitations: Density-Functional Versus Many-Body Green's-Function Approaches. *Rev. Mod. Phys.* **2002**, *74*, 601−659.
(27) Rostgaard, C.; Jacobsen, K. W.; Thygesen, K. S. Fully Self-Consistent GW Calculations for Molecules. *Phys. Rev. B: Condens. Matter Mater. Phys.* **2010**, *81*, 085103.
(28) Ke, S. H. All-Electron GW Methods Implemented in Molecular Orbital Space: Ionization Energy and Electron Affinity of Conjugated Molecules. *Phys. Rev. B: Condens. Matter Mater. Phys.* **2011**, *84*, 205415.
(29) van Setten, M.; Weigend, F.; Evers, F. The GW-Method for Quantum Chemistry Applications: Theory and Implementation. *J. Chem. Theory Comput.* **2013**, *9*, 232−246.
(30) van Setten, M. J.; Caruso, F.; Sharifzadeh, S.; Ren, X.; Scheffler, M.; Liu, F.; Lischner, J.; Lin, L.; Deslippe, J. R.; Louie, S. G.; et al. GW100: Benchmarking G0W0 for Molecular Systems. *J. Chem. Theory Comput.* **2015**, *11*, 5665−5687.
(31) Rice, T. The Effects of Electron-Electron Interaction on the Properties of Metals. *Ann. Phys.* **1965**, *31*, 100−129.
(32) Hedin, L. On Correlation Effects in Electron Spectroscopies and the GW Approximation. *J. Phys.: Condens. Matter* **1999**, *11*, R489.
(33) Shishkin, M.; Marsman, M.; Kresse, G. Accurate Quasiparticle Spectra from Self-Consistent GW Calculations with Vertex Corrections. *Phys. Rev. Lett.* **2007**, *99*, 246403.
(34) Bethe, H. A.; Goldstone, J. Effect of a Repulsive Core in the Theory of Complex Nuclei. *Proc. R. Soc. London, Ser. A* **1957**, *238*, 551−567.
(35) Baym, G.; Kadanoff, L. P. Conservation Laws and Correlation Functions. *Phys. Rev.* **1961**, *124*, 287.
(36) Baym, G. Self-Consistent Approximations in Many-Body Systems. *Phys. Rev.* **1962**, *127*, 1391.
(37) Danielewicz, P. Quantum Theory of Nonequilibrium Processes, I. *Ann. Phys.* **1984**, *152*, 239−304.
(38) Danielewicz, P. Quantum Theory ofNonequilibrium Processes II. Application to Nuclear Collisions. *Ann. Phys.* **1984**, *152*, 305−326.
(39) Bickers, N.; Scalapino, D. Conserving Approximations for Strongly Fluctuating Electron Systems. I. Formalism and Calculational Approach. *Ann. Phys.* **1989**, *193*, 206−251.
(40) Bickers, N.; White, S. Conserving Approximations for Strongly Fluctuating Electron Systems. II. Numerical Results and Parquet Extension. *Phys. Rev. B: Condens. Matter Mater. Phys.* **1991**, *43*, 8044.
(41) Puig von Friesen, M.; Verdozzi, C.; Almbladh, C.-O. Kadanoff-Baym Dynamics of Hubbard Clusters: Performance of Many-Body Schemes, Correlation-Induced Damping and Multiple Steady and Quasi-Steady States. *Phys. Rev. B: Condens. Matter Mater. Phys.* **2010**, *82*, 155108.
(42) Gukelberger, J.; Huang, L.; Werner, P. On the Dangers of Partial Diagrammatic Summations: Benchmarks for the Two-Dimensional Hubbard Model in the Weak-Coupling Regime. *Phys. Rev. B: Condens. Matter Mater. Phys.* **2015**, *91*, 235114.
(43) Liebsch, A. Ni D-Band Self-Energy Beyond the Low-Density Limit. *Phys. Rev. B: Condens. Matter Mater. Phys.* **1981**, *23*, 5203.
(44) Nozieres, P.; Pines, D. Correlation Energy of a Free Electron Gas. *Phys. Rev.* **1958**, *111*, 442.
(45) Romaniello, P.; Bechstedt, F.; Reining, L. Beyond the GW Approximation: Combining Correlation Channels. *Phys. Rev. B: Condens. Matter Mater. Phys.* **2012**, *85*, 155131.
(46) Katsnelson, M. I.; Lichtenstein, A. I. LDA++ Approach to the Electronic Structure of Magnets: Correlation Effects in Iron. *J. Phys.: Condens. Matter* **1999**, *11*, 1037.
(47) Katsnelson, M. I.; Lichtenstein, A. I. Electronic Structure and Magnetic Properties of Correlated Metals. *Eur. Phys. J. B* **2002**, *30*, 9−15.
(48) Zhukov, V.; Chulkov, E.; Echenique, P. GW+ T Theory of Excited Electron Lifetimes in Metals. *Phys. Rev. B: Condens. Matter Mater. Phys.* **2005**, *72*, 155109.
(49) Martin, R. M.; Reining, L.; Ceperley, D. M. *Interacting Electrons - Theory and Computational Approaches*; Cambridge University Press, 2016; p 236.
(50) Martin, R. M.; Reining, L.; Ceperley, D. M. *Interacting Electrons - Theory and Computational Approaches*; Cambridge University Press, 2016; p 238.
(51) Ring, P.; Schuck, P. *The Nuclear Many-Body Problem*; Spinger-Verlag, 1980; p 340.
(52) Shenvi, N.; Van Aggelen, H.; Yang, Y.; Yang, W. Tensor Hypercontracted ppRPA: Reducing the Cost of the Particle-Particle Random Phase Approximation from O (r 6) to O (r 4). *J. Chem. Phys.* **2014**, *141*, 024119.
(53) *QM4D, An In-House Program for QM-MM Simulation*. http://www.qm4d.info (2017).
(54) Dunning, T. H., Jr. Gaussian Basis Sets for Use in Correlated Molecular Calculations. I. The Atoms Boron Through Neon and Hydrogen. *J. Chem. Phys.* **1989**, *90*, 1007.
(55) Woon, D. E.; Dunning, T. H., Jr. Gaussian Basis Sets for Use in Correlated Molecular Calculations. III. The Atoms Aluminum Through Argon. *J. Chem. Phys.* **1993**, *98*, 1358.
(56) Kendall, R. A.; Dunning, T. H., Jr.; Harrison, R. J. Electron Affinities of the First-Row Atoms Revisited. Systematic Basis Sets and Wave Functions. *J. Chem. Phys.* **1992**, *96*, 6796−6806.
(57) Dunning, T. H., Jr.; Harrison, P. J. *Modern Theoretical Chemistry*; Plenum Press, 1977; Vol. 2.
(58) Ren, X.; Tkatchenko, A.; Rinke, P.; Scheffler, M. Beyond the Random-Phase Approximation for the Electron Correlation Energy: The Importance of Single Excitations. *Phys. Rev. Lett.* **2011**, *106*, 153003.
(59) Klimeš, J.; Kaltak, M.; Maggio, E.; Kresse, G. Singles Correlation Energy Contributions in Solids. *J. Chem. Phys.* **2015**, *143*, 102816.
(60) Lin, Y.-S.; Tsai, C.-W.; Chai, J.-D.; Li, G.-D. Long-Range Corrected Hybrid Meta-Generalized-Gradient Approximations with Dispersion Corrections. *J. Chem. Phys.* **2012**, *136*, 154109.
(61) Curtiss, L. A.; Raghavachari, K.; Redfern, P. C.; Rassolov, V.; Pople, J. A. Gaussian-3 (G3) Theory for Molecules Containing First and Second-Row Atoms. *J. Chem. Phys.* **1998**, *109*, 7764−7776.
(62) Curtiss, L. A.; Raghavachari, K.; Redfern, P. C.; Pople, J. A. Assessment of Gaussian-3 and Density Functional Theories for a Larger Experimental Test Set. *J. Chem. Phys.* **2000**, *112*, 7374.
(63) Kawaguchi, K. Fourier Transform Infrared Spectroscopy of the BH3 ν3 Band. *J. Chem. Phys.* **1992**, *96*, 3411−3415.
(64) Willock, D. J. *Molecular Symmetry*; John Wiley and Sons, 2009.
(65) Chong, D.; Gritsenko, O.; Baerends, E. Interpretation of the Kohn-Sham Orbital Energies as Approximate Vertical Ionization Potentials. *J. Chem. Phys.* **2002**, *116*, 1760−1772.
(66) Beste, A.; Vázquez-Mayagoitia, A.; Ortiz, J. V. Direct Delta MBPT(2) Method for Ionization Potentials, Electron Affinities, and Excitation Energies Using Fractional Occupation Numbers. *J. Chem. Phys.* **2013**, *138*, 074101.

DOI: 10.1021/acs.jpclett.7b01275
J. Phys. Chem. Lett. 2017, 8, 3223−3227